

LISAC: Learned Coded Waveform Design for ISAC with OFDM

Chenghong Bian, *Student Member, IEEE*, Yumeng Zhang, *Student Member, IEEE*, Deniz Gündüz, *Fellow, IEEE*

Abstract—We propose a novel deep learning based method to design a coded waveform for integrated sensing and communication (ISAC) system based on orthogonal frequency-division multiplexing (OFDM). Our ultimate goal is to design a coded waveform, which is capable of providing satisfactory sensing performance of the target while maintaining high communication quality measured in terms of the bit error rate (BER). The proposed LISAC provides an improved waveform design with the assistance of deep neural networks for the encoding and decoding of the information bits. In particular, the transmitter, parameterized by a recurrent neural network (RNN), encodes the input bit sequence into the transmitted waveform for both sensing and communications. The receiver employs a RNN-based decoder to decode the information bits while the transmitter senses the target via maximum likelihood detection. We optimize the system considering both the communication and sensing performance. Simulation results show that the proposed LISAC waveform achieves a better trade-off curve compared to existing alternatives.

Index Terms—Integrated sensing and communications (ISAC), deep learning, channel coding.

I. INTRODUCTION

Integrated sensing and communications (ISAC) is attracting increasing attention [1], [2] due to its great potential in mitigating the spectrum shortage and reducing the hardware costs, paving the way for new applications and services in the upcoming 6G networks. Ideal ISAC waveform should balance the achieved communication capacity with the detection/estimation capacities for sensing. Designing an effective ISAC waveform is challenging due to the conflicting requirements of sensing and communications. A foundational study on the trade-off between these two functions, from an information-theoretical perspective, is presented in [2], where the authors show that the sensing-optimal input, based on the Cramér-Rao lower bound (CRLB), features a constant magnitude, while the communication-optimal input follows a random Gaussian distribution, highlighting a so-called “deterministic-random trade-off” between sensing and communications. Rather than designing a new ISAC waveform from scratch, a more pragmatic approach is to employ the

C. Bian and D. Gündüz are with the Department of Electrical and Electronic Engineering, Imperial College London (E-mails: {c.bian22, d.gunduz}@imperial.ac.uk). Y. Zhang is with the Department of Electrical and Computer Engineering, Hong Kong University of Science and Technology, Hong Kong. (E-mail: eeyzhang@ust.hk).

This work received funding from the UKRI for the projects AI-R (ERC Consolidator Grant, EP/X030806/1) and the SNS JU project 6G-GOALS under the EU’s Horizon program Grant Agreement No. 101139232.

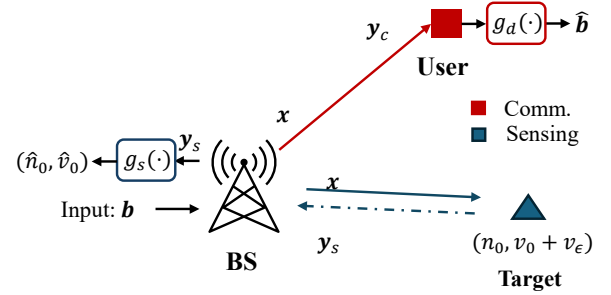


Fig. 1: The considered ISAC system where the BS is sensing one target and communicating with a single user. The BS encodes input bit sequences, b to the LISAC codeword x . The information bits are decoded at the user side while the target parameters are estimated at the BS.

orthogonal frequency division multiplexing (OFDM) waveform for sensing, which has been shown to provide promising estimation precision for radar applications [3]–[5]. A potential solution to the deterministic-random trade-off in OFDM-based ISAC is to use PSK modulation [6], but this limits the communication rate. The superiority of OFDM among communication-centric ISAC waveforms is shown in [7] for both PSK and QAM symbols by studying the ranging performance assuming random information symbols. The authors in [8] propose outlier mean square error (MSE) and outlier probability (OP) as the sensing metrics accounting for OFDM’s resolution limits. However, [8] optimizes the OP metric under an asymptotic channel capacity constraint. Instead of focusing on a uniform distribution, probabilistic constellation shaping is considered in [9] to balance the sensing performance with the channel capacity.

While all the above works evaluate the communication performance through the asymptotic channel capacity achieved through independent and identically distributed (i.i.d.) channel symbols, here we are interested in the practical channel coding performance. The most related prior work is [10], which focus on non-coherent communication with a short block length channel code, and employs a simple DNN model.

In this paper, we develop a deep learning based algorithm, namely, the LISAC model, where a waveform is designed to produce both satisfactory sensing performance and error correction ability based on OFDM. In particular, the encoder

and the decoder of the LISAC model are both parameterized by recurrent neural networks (RNNs). The encoder and the decoder are trained alternatively, where the loss function is a weighted sum of the outlier MSE for sensing and the cross entropy loss between the original bit sequence and the decoder output. Different points on the sensing and communication trade-off can be achieved by employing different weights during training. Unlike in [10], the LISAC model is not confined to the short block length regime. Numerical experiments show that the learned code spreads the transmitted signals across the I/Q plane when communication performance is the priority, while it converges to a mixture between PSK and amplitude modulation when the sensing performance becomes important. Our results show that the proposed learned coded-modulation scheme achieves a better sensing and communication trade-off compared with the existing methods.

II. PROBLEM FORMULATION

In this section, we introduce the LISAC framework where channel coded symbols are utilized to perform user communication and target sensing simultaneously.

A. Communication model

As shown in Fig. 1, the transmitter takes the information bit sequence, $\mathbf{b} \in \{0, 1\}^L$, as input and produces the complex OFDM signal in the frequency domain, $\mathbf{X} \in \mathbb{C}^{K \times M}$:

$$\mathbf{X} = f_s(\mathbf{b}), \quad (1)$$

where $f_s(\cdot)$ represents the encoding function while K, M denote the number of OFDM subcarriers and the number of OFDM symbols, respectively. A power constraint is imposed on the OFDM symbols as:

$$\|\mathbf{X}\|_F^2 \leq KM. \quad (2)$$

The subcarrier signals at the m -th OFDM symbol, $\mathbf{X}[:, m]$, is transformed to the time-domain signals, defined as $\mathbf{x}[:, m]$ via IFFT, which is further concatenated with a length- K_G cyclic prefix (CP) for transmission.

We assume there is only one line-of-sight (LoS) path with a unit channel gain between the transmitter and the receiver. Moreover, for simplicity, the receiver is considered to be static leading to flat frequency response¹ for each of the OFDM symbols.

After removing the CP and applying FFT, the received signal can be expressed as:

$$\mathbf{Y}_c = \mathbf{X} + \mathbf{Z}_c, \quad (3)$$

where $\mathbf{Z}_c \in \mathbb{C}^{K \times M}$ denotes the additive white Gaussian noise (AWGN) in the communication link, satisfying $\mathbf{Z}_c[i, j] \sim \mathcal{CN}(0, \sigma_c^2)$ and the signal-to-noise-ratio (SNR) for the communication link is $\text{SNR}_c \triangleq 1/\sigma_c^2$.

The receiver decodes the noisy signal, \mathbf{Y}_c into a bit sequence, $\hat{\mathbf{b}}$:

$$\hat{\mathbf{b}} = g_d(\mathbf{Y}_c), \quad (4)$$

¹We note that the proposed scheme is also applicable to frequency selective channel which will be shown in the journal version.

where $g_d(\cdot)$ denotes the decoding function, which first transforms \mathbf{Y}_c into a vector and then demodulates and decodes the vector. The BER is utilized as the communication performance metric defined as:

$$\text{BER} = \frac{1}{L} \mathbb{E} \left[\sum_{i=1}^L \mathbf{1}(\mathbf{b}_i \neq \hat{\mathbf{b}}_i) \right], \quad (5)$$

where $\mathbf{1}(\cdot)$ represents the indicator function.

B. Sensing model

We then describe the proposed sensing model, assuming a single target at a distance R from the transmitter moving at a speed v . As a result, the received echo signal is delayed by $\tau = 2R/c$ with a Doppler shift of $f_D \triangleq f_c(2v/c)$, where f_c is the carrier frequency. The bandwidth of the OFDM symbol, B , corresponds to a delay resolution of $\Delta\tau = 1/B$. The duration of the OFDM symbol is $T = (K + K_G)/B$ leading to a Doppler resolution of $\Delta f_D = \frac{B}{(K + K_G)M}$. The delay and Doppler of the target, τ and f_D , can be represented using $\Delta\tau$ and Δf_D , respectively:

$$\tau = (n_0 + n_\epsilon)\Delta\tau, \quad (6)$$

$$f_D = (v_0 + v_\epsilon)\Delta f_D, \quad (7)$$

where (n_0, v_0) are the integer delay and Doppler to be estimated. The fractional delay and Doppler, $n_\epsilon \in (0, 1)$ and $v_\epsilon \in (-1/2, 1/2)$, are often out of the scope of estimation due to the radar resolution issues. However, their effects on the estimation of the parameters of interest, (n_0, v_0) , need to be taken into account.

After removing the CP, the time-domain signal at the n -th time slot of the m -th OFDM symbol can be expressed as:

$$\mathbf{y}[n, m] \approx a\mathbf{x}[n - n_0, m]e^{j2\pi\frac{(v_0 + v_\epsilon)m}{M}} + \mathbf{w}[n, m], \quad (8)$$

where a is the complex gain of the radar channel assumed to remain constant during the OFDM block, while $\mathbf{x}[n - n_0, m]$ is a circular shifted version of the transmitted signal $\mathbf{x}[n, m]$ by n_0 due to the delay². The $e^{j2\pi\frac{(v_0 + v_\epsilon)m}{M}}$ term represents the phase shift of the m -th OFDM symbol due to the Doppler effect. Finally, $\mathbf{w}[n, m] \in \mathcal{CN}(0, \sigma_s^2)$ denotes the AWGN term, and the SNR of the sensing link is defined as $\text{SNR}_s \triangleq 1/\sigma_s^2$.

We then convert the time-domain signal in (8) to the frequency domain via K -point FFT:

$$\mathbf{Y}[k, m] = a\mathbf{X}[k, m]e^{j2\pi\frac{(v_0 + v_\epsilon)m}{M}} e^{-j2\pi\frac{n_0 k}{K}} + \mathbf{W}[k, m], \quad (9)$$

where $\mathbf{W}[k, m] \sim \mathcal{CN}(0, \sigma_s^2)$ is the noise in the frequency domain.

²The fractional term of the delay, n_ϵ is omitted because we assume perfect time synchronization at the receiver that eliminates the effect of n_ϵ .

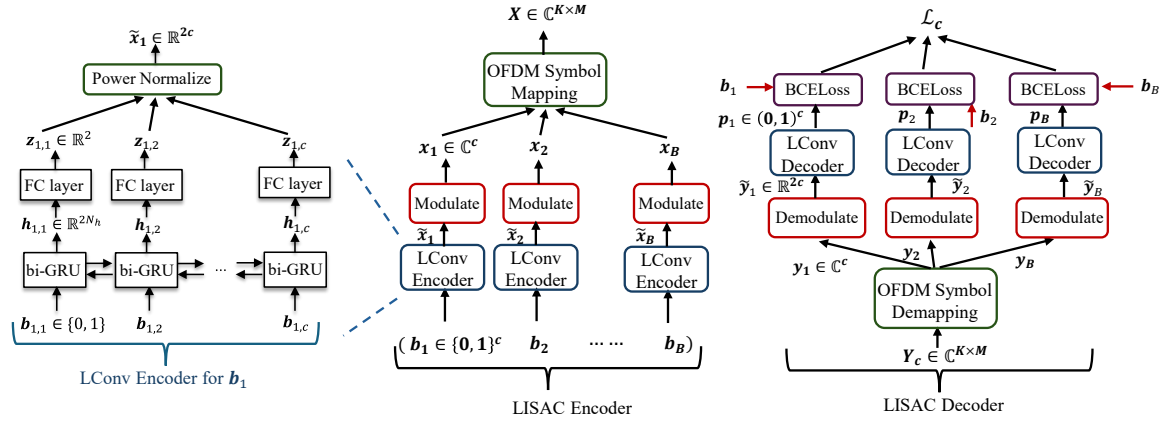


Fig. 2: Illustration of the neural network architecture of the LISAC encoder and decoder. In particular, the LISAC encoder is comprised of a rate-1/2 learning-based convolutional encoder (LConv), a modulation block and the OFDM symbol mapping block which maps the B symbols to M OFDM symbols. The LISAC receiver decodes the information bits from its received signal, \mathbf{Y}_c . The BCE loss is adopted as a loss function for the communication part.

1) *Maximum likelihood (ML) estimation*: We then elaborate the ML estimator of the interested target parameters, i.e., (n_0, v_0) . The log-likelihood function can be expressed as:

$$L(\mathbf{Y}|n_0, v_0, v_\epsilon, a) \propto - \sum_{k=0}^{K-1} \sum_{m=0}^{M-1} |\mathbf{Y}[k, m] - \mathbf{X}[k, m] e^{j2\pi \frac{(v_0+v_\epsilon)m}{M}} e^{-j2\pi \frac{n_0 k}{K}}|^2. \quad (10)$$

By expanding the right-hand-side (RHS) of (10), the ML estimator can be expressed as:

$$\begin{aligned} (\hat{n}_0, \hat{v}_0) &= \arg \max_{(n, v)} \left| \underbrace{\sum_{m, k} p_{k, m} e^{j2\pi \frac{n k}{K}} e^{-j2\pi \frac{(v+v_\epsilon)m}{M}} + \widetilde{\mathbf{W}}[n, v]}_{r_{n, v, v_\epsilon}} \right| \\ &= \arg \max_{(n, v)} |\gamma_{n, v, v_\epsilon}|, \end{aligned} \quad (11)$$

where $p_{k, m} \triangleq |\mathbf{X}[k, m]|^2$ is the power of the transmit signal for the k -th subcarrier at the m -th OFDM symbol, $\gamma_{n, v, v_\epsilon}$ is defined as $\gamma_{n, v, v_\epsilon} \triangleq r_{n, v, v_\epsilon} + \widetilde{\mathbf{W}}[n, v]$ while $\widetilde{\mathbf{W}}[n, v], n \in [0, K_G - 1], v \in [-M/2, M/2 - 1]$ is defined as:

$$\widetilde{\mathbf{W}}[n, v] \triangleq A^{-1} \sum_{m, k} \mathbf{W}[k, m] \mathbf{X}^*[k, m] e^{-j2\pi \frac{n k}{K}} e^{j2\pi \frac{v m}{M}}, \quad (12)$$

where $A \triangleq |a|$ denotes the amplitude for the complex gain. It can be noticed from (11) that the ML estimator performance is determined by the power of the waveform, i.e., $p_{k, m}$.

2) *Outlier MSE*: Due to the noise and the fractional Doppler, v_ϵ , the ML detector output, (\hat{n}_0, \hat{v}_0) might deviate from the ground truth, (n_0, v_0) . As in [8] and [11], we adopt the outlier MSE, denoted as E_o , to quantify the expected l_2 -distance between (\hat{n}_0, \hat{v}_0) and (n_0, v_0) . Without loss of generality, we assume $(n_0, v_0) = (0, 0)$ and E_o is expressed as:

$$E_o \triangleq \mathbb{E}_{v_\epsilon} (\hat{n}_0^2 + \hat{v}_0^2). \quad (13)$$

III. THE PROPOSED LISAC FRAMEWORK

As analyzed in Section II, though [8] provides an insightful solution to the waveform design, i.e., $p_{k, m}$, using conventional optimization methods such as alternating direction method of multipliers (ADMM), the authors do not take the error correction ability of the optimized waveform into account. It is difficult to incorporate the BER performance into the conventional optimization frameworks; therefore, we employ a learning-based approach in this paper to overcome this difficulty.

A. LISAC encoder

We first discuss the neural network architecture of the LISAC encoder. In particular, the input bit sequence, $\mathbf{b} \in \{0, 1\}^L$ is first partitioned into B blocks, i.e., $\mathbf{b} = [\mathbf{b}_1, \mathbf{b}_2, \dots, \mathbf{b}_B]$, where each block is of length- C , i.e., $\mathbf{b}_b \in \{0, 1\}^C$, satisfying $BC = L$. All the B blocks are processed by the LISAC encoder simultaneously.

Take the first block, \mathbf{b}_1 as an example. As shown in the middle of Fig. 2, \mathbf{b}_1 is fed to the LConv encoder to obtain a real-valued codeword, $\tilde{\mathbf{x}}_1 \in \mathbb{R}^{2C}$. The neural network architecture of the LConv encoder shown in the left of Fig. 2 is comprised of non-linear transformation modules and a power normalization module. The neural network parameters of the LISAC encoder are denoted as Θ_e . In particular, the bidirectional-GRU (bi-GRU) block of the non-linear transformation modules at the c -th time step takes the c -th bit, $\mathbf{b}_{1, c}$ as input and outputs a latent vector, $\mathbf{h}_{1, c} \in \mathbb{R}^{2N_h}, c \in [1, C]$:

$$\{\mathbf{h}_{1, c}\}_{c \in [1, C]} = \text{bi-GRU}(\{\mathbf{b}_{1, c}\}_{c \in [1, C]}), \quad (14)$$

where N_h denotes the hidden dimension of the bi-GRU block and 2 is due to the forward and backward directions. Then, a fully connected (FC) layer is applied to each of the latent vectors, $\mathbf{h}_{1, c}$ to generate $\mathbf{z}_1 = [z_{1, 1}^\top, z_{1, 2}^\top, \dots, z_{1, C}^\top]^\top$, where $z_{1, c} \in \mathbb{R}^2$. The codeword $\mathbf{z}_1 \in \mathbb{R}^{2C}$ can be interpreted as the

codeword of a rate-1/2 channel code. We then apply power normalization to \mathbf{z}_1 to generate the LConv encoder output, $\tilde{\mathbf{x}}_1 \in \mathbb{R}^{2C}$:

$$\begin{aligned} \tilde{\mathbf{x}}_1 &= \frac{\mathbf{z}_1 - \mu}{\sqrt{2\sigma}}, \\ \mu &= \mathbb{E}(\mathbf{z}_{1,c}); \quad \sigma^2 = \mathbb{E}(\mathbf{z}_{1,c} - \mu)^2, \end{aligned} \quad (15)$$

where μ, σ are calculated by averaging over sufficient number of \mathbf{z}_1 realizations during training and $\sqrt{2}$ is introduced to satisfy the power constraint in (2).

We modulate the power normalized symbols, $\tilde{\mathbf{x}}_1$, to a complex-valued codeword, $\mathbf{x}_1 \in \mathbb{C}^C$. The modulation process is achieved by taking the first C elements of $\tilde{\mathbf{x}}_1$ as the real part and the remaining elements as the imaginary part:

$$\mathbf{x}_1 = \tilde{\mathbf{x}}_{1,1:C} + j\tilde{\mathbf{x}}_{1,C:2C}. \quad (16)$$

After obtaining B such modulated codewords, $[\mathbf{x}_1, \dots, \mathbf{x}_B]$, we map them to M OFDM symbols each with K subcarriers to form the transmitted signal satisfying $BC = KM$. Two different OFDM mapping strategies are evaluated, where the first one loads the data in a column-first fashion while the second one performs row-first data loading. Since it is shown in the experiments that the two data loading schemes yield similar performance, we use the first strategy throughout the paper.

B. LISAC decoder

We illustrate the LISAC decoder on the RHS of Fig. 2. In particular, the received signal \mathbf{Y}_c is demapped to B symbols, $[\mathbf{y}_1, \dots, \mathbf{y}_B]$. Each of the symbols, \mathbf{y}_b , is demodulated to a real-valued vector, $\tilde{\mathbf{y}}_b \in \mathbb{R}^{2C}$, by concatenating the real and imaginary parts of \mathbf{y}_b . The real-valued vector, $\tilde{\mathbf{y}}_b$ is further fed to the LConv decoder to generate the probability vector, $\mathbf{p}_b \triangleq [p_{b,1}, \dots, p_{b,C}] \in (0, 1)^C$. In particular, $\tilde{\mathbf{y}}_b$ is partitioned into C blocks, $\tilde{\mathbf{y}}_b = [\tilde{\mathbf{y}}_{b,1}, \dots, \tilde{\mathbf{y}}_{b,C}]$ with $\tilde{\mathbf{y}}_{b,c} \in \mathbb{R}^2$ before feeding into the LConv decoder. The LConv decoder also consists of bi-GRU blocks and a FC layer, parameterized by Θ_d . However, compared with the LConv encoder, its bi-GRU blocks take a 2d vector as input and its FC layer produces a scalar output, $p_{b,c} \in (0, 1)$.

C. Training of the LISAC system

Next, we present the training procedure of the LISAC system. To begin with, the loss functions for both communication and sensing are introduced.

1) *Loss functions*: For the receiver, we adopt the widely used binary cross entropy (BCE) loss in the literature [12], which can be expressed as:

$$\mathcal{L}_c = - \sum_b \sum_c (b_{b,c} \log_2(p_{b,c}) + (1 - b_{b,c}) \log_2(1 - p_{b,c})), \quad (17)$$

where p_b is the LISAC decoder output.

The loss function for target sensing is more complicated. A naive solution is to directly adopt the outlier MSE, E_o , defined in (13). However, the acquisition of the indices, (\hat{n}_0, \hat{v}_0) , involves argmax operation in (11), which is non-differentiable.

Algorithm 1: Training algorithm for the LISAC encoder and decoder.

Input : $K, M, B, C, \lambda, N_e, N_d, N_{epoch}$

Output: Optimized $\{\Theta_e, \Theta_d\}$

```

for  $n = 1$  to  $N_{epoch}$  do
  Fix LISAC decoder parameters,  $\Theta_d$ .
  for  $n_e = 1$  to  $N_e$  do
    Randomly sample
       $\mathbf{b}_b \in \{0, 1\}^C, \forall b \in [1, B]; v_\epsilon \sim \mathcal{U}(-1/2, 1/2)$ .
       $\tilde{\mathbf{x}}_b = \text{LConvEncode}(\mathbf{b}_b)$ ,
       $\mathbf{x}_b = \text{Modulate}(\tilde{\mathbf{x}}_b)$ ,
       $\mathbf{X} = \text{OFDMSymMap}(\{\mathbf{x}_b\}_{b \in [1, B]})$ ,
       $\triangleright$  LISAC encoding.
       $(\mathbf{Y}_c, \mathbf{Y}_S) \leftarrow \text{Eqn. (3), Eqn. (9)}$ 
       $\{\mathbf{y}_b\}_{b \in [1, B]} \leftarrow \text{OFDMSymDeMap}(\mathbf{Y}_c)$ ,
       $\tilde{\mathbf{y}}_b \leftarrow \text{DeModulate}(\mathbf{y}_b)$ ,
       $\mathbf{p}_b \leftarrow \text{LConvDecode}(\tilde{\mathbf{y}}_b)$ ,
       $\triangleright$  LISAC decoding.
       $\mathcal{L}_c \leftarrow \text{Eqn. (17)}; \quad \mathcal{L}_s \leftarrow \text{Eqn. (18) using } v_\epsilon$ .
      Optimize  $\Theta_e$  using  $\mathcal{L} = \mathcal{L}_c + \lambda \mathcal{L}_s$ .
  Fix LISAC encoder parameters,  $\Theta_e$ .
  for  $n_d = 1$  to  $N_d$  do
    Generate  $\{\mathbf{b}_b, \mathbf{p}_b\}_{b \in [1, B]}$  repeating line 4-12.
     $\mathcal{L}_c \leftarrow \text{Eqn. (17)}$ .
    Optimize  $\Theta_d$  using  $\mathcal{L}_c$ .

```

To this end, we consider a proxy loss function, \mathcal{L}_s , which is expressed as:

$$\mathcal{L}_s = \mathbb{E}_{v_\epsilon} \sum_{(n,v) \neq (0,0)} (n^2 + v^2) P_{(0,0) \rightarrow (n,v)}(v_\epsilon), \quad (18)$$

where we assume the ground truth $(n_0, v_0) = (0, 0)$ and $P_{(0,0) \rightarrow (n,v)}(v_\epsilon)$ is the pairwise outlier probability, defined following the maximum likelihood principle:

$$P_{(0,0) \rightarrow (n,v)}(v_\epsilon) \triangleq P(|\gamma_{n,v,v_\epsilon}| > |\gamma_{0,0,v_\epsilon}|), \quad (19)$$

where γ_{n,v,v_ϵ} is defined in (11). The exact formula of $P_{(0,0) \rightarrow (n,v)}(v_\epsilon)$ is given in [8] and is omitted in this paper due to the page limit. Compared to the outlier MSE in (13), \mathcal{L}_s provides a ‘soft’ measurement on how the estimated delay and doppler indices, (n, v) , deviate from the ground truth. Note that, even though \mathcal{L}_s is not exactly the outlier MSE, we can still achieve satisfactory performance as we will see in the simulations in Section IV.

The overall loss function can be expressed as:

$$\mathcal{L} = \mathcal{L}_c + \lambda \mathcal{L}_s, \quad (20)$$

where λ determines whether the learned waveform is sensing-oriented or communication-oriented. In particular, with a large λ value, one would expect a satisfactory sensing performance with a high BER value, and vice versa for a small λ value.

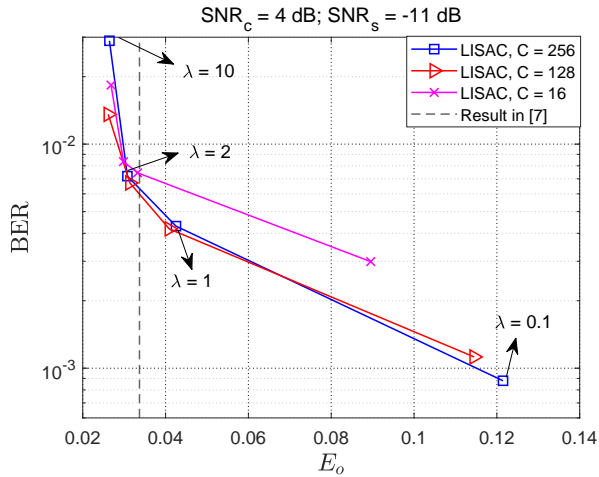


Fig. 3: Communication and sensing trade-off with different codeword lengths, C . Different trade-off points are achieved with varying $\lambda \in \{0.1, 1, 2, 10\}$. We also provide the performance achieved by the conventional convolutional code.

2) *Training methodology*: To avoid getting stuck on local optima, we train the LISAC encoder and decoder alternatively. In particular, we optimize the LISAC encoder for N_e iterations using the overall loss function, \mathcal{L} defined in (20), with Θ_d fixed. Next, we fix Θ_e and train LISAC decoder using only \mathcal{L}_c for N_d iterations. In general, we have $N_d > N_e$ as the LISAC decoder is harder to optimize. A large batch size is adopted which is essential for achieving a satisfactory decoding performance. The overall training algorithm is summarized in Algorithm 1.

IV. NUMERICAL EXPERIMENTS

A. Parameter Settings and Training Details

Unless otherwise mentioned, we consider a rate-1/2 LISAC codeword and adopt the modulation scheme detailed in (16) leading to a spectrum efficiency equals to one.

For different numbers of OFDM subcarriers, K , and OFDM symbols, M , we vary the code length, C , and the number of input bit sequences, B , to satisfy the condition, $BC = KM$. The batch size is set to 10^3 , and the learning rate for both LISAC encoder and decoder is set to 10^{-3} . Adam optimizer is adopted and the model is trained for 100 epochs. For each epoch, the LISAC encoder is optimized $N_e = 2 \times 10^4$ times, while the LISAC decoder is updated $N_d = 5 \times 10^4$ times. The LISAC encoder and decoder are trained at fixed SNR_c and SNR_s but evaluated at different SNR_c and SNR_s values. The rate-1/2 convolutional code with constraint length of 7 with polynomial generator, (171, 133) is adopted as the baseline. For a fair comparison with the proposed LISAC scheme, the rate-1/2 convolutional code is QPSK modulated to provide a spectral efficiency equals to one.

B. Performance Evaluation

1) *Characterization of the communication and sensing trade-off*: We first characterize the communication and sensing

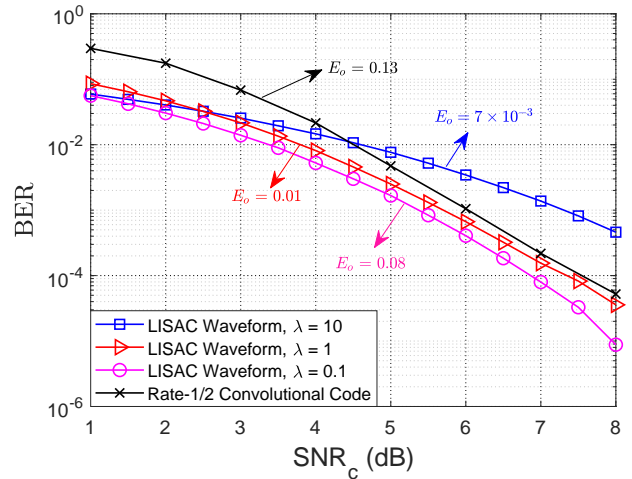


Fig. 4: The BER comparison between the LISAC waveform trained under different λ values with the 1/2-rate convolutional code using QPSK modulation.

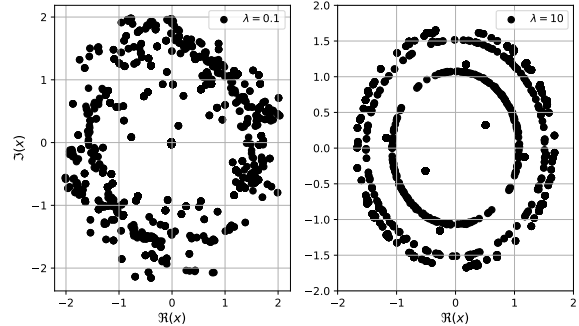


Fig. 5: Visualization of the learned codeword, x defined in (15) with the block length, $C = 8$. The x/y -axis's are the real/imaginary parts of x , respectively. Visualizations for $\lambda = 0.1$ (left) and $\lambda = 10$ (right) are provided.

trade-off in terms of the BER and the sensing MSE, E_o , defined in (13). In this simulation, we consider the OFDM setting with $K = 32$, $M = 8$, the communication and sensing SNRs are set to $\text{SNR}_c = 4$ dB and $\text{SNR}_s = -11$ dB, respectively. Different codeword lengths, $C = \{16, 128, 256\}$ are considered and the corresponding number of blocks are $B = \{16, 2, 1\}$. For a specific (B, C) setup, we train four distinct LISAC models with different $\lambda \in \{0.1, 1, 2, 10\}$ values. As a result, 12 models are obtained, each yielding a distinct trade-off between BER and sensing MSE value as plotted in Fig. 3. The dashed line in the same figure represents the sensing performance achieved by the analytical optimization method illustrated in [8] where the authors adopt QPSK modulation and assign different powers to the OFDM symbols for satisfactory sensing performance.

We can observe from the figure that the BER performance with a large C is better by comparing the LISAC models with

different C parameters at $\lambda = 0.1$.³ This is intuitive as the longer the block length the better the error correction ability. However, when λ becomes larger, e.g., $\lambda = 10$, the LISAC waveform with $C = 256$ yields the worst BER performance. This is attributed to the fact that, for $C = 256$, it is hard for the LISAC encoder to learn a length-256 codeword that is good for both sensing and error correction. In particular, the neural network is likely to get stuck at a local optima dominated by the sensing performance, instead of the global optima, which would achieve a lower BER, albeit with limited impact on the loss function. When the block length reduces, e.g., $C = 128$, it would be easier for the LISAC encoder to reach the global optimal. We observe that, setting $C = 128$ always yields a satisfactory performance over all λ values. We further note that the BER performance of the baseline scheme in [8] is 0.13, which is significantly outperformed by all the LISAC models due to the non-uniform power allocation over the M different OFDM symbols [8]. It can be seen in the figure that the LISAC system with $\lambda > 2$ yields even smaller sensing MSE compared with the benchmark (specifically designed for radar sensing), which is plausible as the analytical optimization method may converge to a sub-optimal solution.

2) *BER comparison with a conventional coded modulation scheme:* Next, we consider the OFDM setting with $K = 32, M = 16$. The corresponding coding scheme adopts $C = 128, B = 4$. Three different models achieving different communication and sensing trade-offs are trained for $\lambda \in \{0.1, 1, 10\}$ values and fixed sensing SNR, $\text{SNR}_s = -13$ dB. The relative performance between the LISAC waveform and the conventional convolutional code evaluated for $\text{SNR} \in [1, 8]$ dB is shown in Fig. 4.

As can be seen, the LISAC waveform with $\lambda = 0.1$ has the best BER performance yet the worst sensing performance, i.e., E_o , compared to the models with $\lambda = \{1, 10\}$. This is intuitive as the LISAC encoder and decoder pair with $\lambda = 0.1$ are optimized with an emphasis on communications. When λ grows, the communication performance degrades yet the outlier MSE decreases. All the LISAC waveforms outperform the conventional convolution code baseline in terms of outlier MSE. It is shown in the figure that the LISAC models with $\lambda = \{0.1, 1\}$ outperform the baseline in terms of BER over the whole considered SNR range.

3) *Visualization of the learned codewords:* Finally, we visualize the symbols employed by the learned codewords to provide more insights on the properties of the coded modulation scheme. In this simulation, we consider the same OFDM setup as in Fig. 3. The block length is set to $C = 8$, corresponding to $2^C = 64$ different codewords⁴. Each of the 2^C codewords has $C = 8$ complex symbols and in total, $C2^C$ number of complex symbols are shown altogether in each of the plots in Fig. 5. The two plots correspond to different LISAC waveforms trained under $\lambda = \{0.1, 10\}$.

³This is plausible because the waveform with $\lambda = 0.1$ corresponds to a communication-oriented one.

⁴Though in practice, we adopt much larger C for better error correction ability. In this simulation, we set $C = 8$ to simplify the visualization.

As can be seen in the figure, the symbols corresponding to $\lambda = 0.1$ appear to be more spread across the I/Q plane, in order to carry more information while minimizing the BER by maximizing the distance between codewords. The codewords obtained with $\lambda = 10$, on the other hand, are concentrated on several co-centric circles. Since the elements belonging to the same circle have the same amplitude, information can only be embedded on the phase of the element. Thus, the waveform trained with $\lambda = 10$ has less satisfactory BER performance as verified in Fig. 3. On the other hand, there are only few possible amplitudes, $p_{k,m}$, available for the waveform with $\lambda = 10$ leading to a better sensing performance. This aligns with the intuition that deterministic amplitude signals are well suited for sensing.

V. CONCLUSION

In this paper, a novel LISAC framework is proposed to achieve satisfactory sensing and communication performance by a fully-learnable coded waveform. The LISAC encoder and the decoder are parameterized by RNNs, and are trained alternatively in an end-to-end fashion. Different LISAC models are trained to obtain different sensing and communication trade-offs. Numerical experiments are carried out to illustrate the effectiveness of the proposed LISAC framework.

REFERENCES

- [1] F. Liu, Y. Cui, C. Masouros, J. Xu, T. X. Han, Y. C. Eldar, and S. Buzzi, "Integrated sensing and communications: Toward dual-functional wireless networks for 6G and beyond," *IEEE J. Sel. Areas in Commun.*, vol. 40, no. 6, pp. 1728–1767, 2022.
- [2] Y. Xiong, F. Liu, Y. Cui, W. Yuan, T. X. Han, and G. Caire, "On the fundamental tradeoff of integrated sensing and communications under Gaussian channels," *IEEE Trans. on Info. Theory*, vol. 69, no. 9, pp. 5723–5751, 2023.
- [3] C. R. Berger, B. Demissie, J. Heckenbach, P. Willett, and S. Zhou, "Signal processing for passive radar using OFDM waveforms," *IEEE J. Sel. Topics in Signal Process.*, vol. 4, no. 1, pp. 226–238, 2010.
- [4] M. Braun, C. Sturm, and F. K. Jondral, "Maximum likelihood speed and distance estimation for OFDM radar," in *IEEE Radar Conf.*, 2010, pp. 256–261.
- [5] C. Bian, K. Meng, H. Wu, and D. Gündüz, "Sparse regression codes for integrated passive sensing and communications," *arXiv:2411.05531*, 2024.
- [6] R. F. Tigrek, W. J. A. De Heij, and P. Van Genderen, "OFDM signals as the radar waveform to solve doppler ambiguity," *IEEE Trans. Aerosp. Electron. Syst.*, vol. 48, no. 1, pp. 130–143, 2012.
- [7] F. Liu, Y. Zhang, Y. Xiong, S. Li, W. Yuan, F. Gao, S. Jin, and G. Caire, "OFDM achieves the lowest ranging sidelobe under random ISAC signaling," *arXiv:2407.06691*, 2024.
- [8] Y. Zhang, S. Aditya, and B. Clerckx, "Input distribution optimization in OFDM dual-function radar-communication systems," *IEEE Trans. on Signal Process.*, 2024.
- [9] Z. Du, F. Liu, Y. Xiong, T. X. Han, Y. C. Eldar, and S. Jin, "Reshaping the ISAC tradeoff under OFDM signaling: A probabilistic constellation shaping approach," *IEEE Trans. on Signal Process.*, 2024.
- [10] M. Kim, T. Jahani-Nezhad, S. Lit, R. F. Schaefer, and G. Caire, "Short-length code designs for integrated sensing and communications using deep learning," in *IEEE Intl. Conf. on Commun.*, 2024, pp. 3536–3541.
- [11] F. Athley, "Threshold region performance of maximum likelihood direction of arrival estimators," *IEEE Trans. on Signal Process.*, vol. 53, no. 4, pp. 1359–1373, 2005.
- [12] H. Kim, Y. Jiang, R. B. Rana, S. Kannan, S. Oh, and P. Viswanath, "Communication algorithms via deep learning," in *International Conference on Learning Representations*, 2018.